

Original research

Protective phenotypes of club cells and alveolar macrophages are favored as part of endotoxin-mediated prevention of asthma

Luciana N García¹, Carolina Leimgruber¹, Elisa M Uribe Echevarría¹, Patricio L Acosta², Jorge M Brahamian², Fernando P Polack^{2,3}, María S Miró⁴, Amado A Quintar¹, Claudia E Sotomayor⁴ and Cristina A Maldonado¹

¹Instituto de Investigaciones en Ciencias de la Salud (INICSA), CONICET and Centro de Microscopía Electrónica- Facultad de Ciencias Médicas, Universidad Nacional de Córdoba, Enrique Barros esq. Enfermera Gordillo, Ciudad Universitaria X5000HRA, Córdoba, Argentina; ²Fundación INFANT, Gavilan 94 C1406ABC, Capital Federal, Buenos Aires, Argentina; ³Department of Pediatrics, Vanderbilt University, MCN, Vanderbilt University, Nashville, TN 37232, USA; ⁴Centro de Investigación en Bioquímica Clínica e Inmunología (CIBICI), Facultad de Ciencias Químicas, Universidad Nacional de Córdoba, Haya de la Torre y Medina Allende (X5000HRA), Ciudad Universitaria, Córdoba, Argentina

Corresponding author: Cristina A Maldonado. Email: cmaldon@cmefcm.uncor.edu

Abstract

Atopic asthma is a chronic allergic disease that involves T-helper type 2 (Th2)-inflammation and airway remodeling. Bronchiolar club cells (CC) and alveolar macrophages (AM) are sentinel cells of airway barrier against inhaled injuries, where allergy induces mucous metaplasia of CC and the alternative activation of AM, which compromise host defense mechanisms and amplify Th2-inflammation. As there is evidence that high levels of environmental endotoxin modulates asthma, the goal of this study was to evaluate if the activation of local host defenses by Lipopolysaccharide (LPS) previous to allergy development can contribute to preserving CC and AM protective phenotypes. Endotoxin stimulus before allergen exposition reduced hallmarks of allergic inflammation including eosinophil influx, Interleukin-4 and airway hyperreactivity, while the T-helper type 1 related cytokines IL-12 and Interferon- γ were enhanced. This response was accompanied by the preservation of the normal CC phenotype and the anti-allergic proteins Club Cell Secretory Protein (CCSP) and Surfactant-D, thereby leading to lower levels of CC metaplasia and preventing the increase of the pro-Th2 cytokine Thymic stromal lymphopoietin. In addition, classically activated alveolar macrophages expressing nitric oxide were promoted over the alternatively activated ones that expressed arginase-1. We verified that LPS induced a long-term overexpression of CCSP and the innate immune markers Toll-like receptor 4, and Tumor Necrosis Factor- α , changes that were preserved in spite of the allergen challenge. These results demonstrate that LPS pre-exposition modifies the local bronchioalveolar microenvironment by inducing natural anti-allergic mechanisms while reducing local factors that drive Th2 type responses, thus modulating allergic inflammation.

Keywords: Club cell, alveolar macrophage, asthma, pulmonary host defense

Experimental Biology and Medicine 2014; 0: 1–13. DOI: 10.1177/1535370214562338

Introduction

Asthma is a chronic inflammatory disease that involves immune, neuronal, and respiratory tissue cells. This disease is characterized by the priming of allergen-specific CD4⁺ Th2 cells, the production of Interleukin-4 (IL-4), IL-13, and IL-5, and B cell secretion of Immunoglobulin E, leading to airway hyperreactivity and obstruction.¹ The repetitive exposure to allergens produces long-term remodeling in lung tissue, which results in the histological hallmarks of asthma, such as mucus hypersecretion, smooth muscle hyperplasia, subepithelial fibrosis, blood

vessel proliferation and the infiltration of inflammatory cells. Consequently, remodeling process alters the structure and function of the airways.²

Although in the bronchoalveolar space, the eosinophils, basophils, mast cells, and dendritic cells are activated in atopic individuals after being exposed to allergens, the epithelial barrier and alveolar macrophages (AM) are the first cells that come into contact with inhaled antigens.^{3,4} Related to this, the majority of the cytokines and chemokines that initiate the immune response in asthma (IL-4, IL-13, CC-chemokine ligand 11, thymic stromal lymphopoietin-TSLP, among others) are secreted by airway epithelial cells and

macrophages.⁵ Particularly, TSLP has emerged as an important epithelial cell-derived cytokine implicated in orchestrating the inflammatory process seen in asthma and other atopic diseases.^{6–8}

The involvement of the epithelium at the inception of asthma pathogenesis represents an abnormal response of the airway epithelial cell role at the regulation of both the innate and adaptive immune responses by expressing several molecules such as microbicidal substances and immunomodulatory proteins. On the other hand, epithelial cells are together with AM the main cell populations in murine airways that are Toll-like receptors (TLR) competent.^{3,9,10} Therefore, epithelial cells are situated at the crossroads of the antibacterial host defense and allergic inflammation, with the manner in which they are primed resulting in either the maintenance or alteration of the lung homeostasis. This plasticity to change their physiology in response to different microenvironments is clearly illustrated by bronchiolar club cells (CC), which are the principal secretory cells at this level. Besides being committed to the local homeostasis through cell renewal and xenobiotic metabolism, CC also actively contributes to the host defense through the secretion of monocyte and neutrophil chemoattractants, the collectin surfactant protein (SP)-D and the anti-inflammatory-immunomodulatory club cell secretory protein (CCSP).^{11,12} Interestingly, SP-D and CCSP have been shown to play a direct role in suppressing allergic inflammation through the reduction of Th2 cytokines, pulmonary eosinophilia and allergen-induced CD4+Th2 cell proliferation, with both proteins inciting Th1 cytokines, thus counterbalancing allergic inflammation.^{13,14} Furthermore, CC also respond actively to Th2-inflammation by producing eotaxin and undergoing epidermal growth factor receptor (EGFR)-mediated mucus metaplasia.^{15–17} Related to this, our previous findings indicated that CC mucous metaplasia leads to a marked decrease in CCSP and SP-D secretion.^{18,19}

In common with epithelial cells, AM are also plastic cells involved in the first line of defense against inhaled agents, which are endowed with a high phagocytic and microbicidal potential and a lower expression of MHC class II molecules.^{4,20} Th2 inflammation induces a wound-healing phenotype, named alternatively activated macrophages (AAM), which amplifies asthma remodeling.²¹ In response to allergy, it has been described that AM become AAM, displaying a high arginase-1 (Arg 1) activity that produces chronic inflammation mediators and precursors of the extracellular matrix.²² Instead, Th1 conditions promote a microbicidal phenotype called classically activated macrophages (CAM), which produce pro-inflammatory cytokines and mediators such as nitric oxide (NO), resulting from inducible NO synthase (iNOS).²¹ At the molecular level, these dissimilar activation phenotypes are linked to the differential upregulation of the L-arginine-consuming enzymes iNOS and Arg-1.²³

The “hygiene hypothesis”²⁴ postulated that the lack of early microbial challenges, caused by the modern life style, increases the propensity of atopic children to develop a Th2-cell-type response to a variety of common environmental allergens.²⁵ Strikingly, bacterial compounds and

endotoxins have been reported to be able to counterbalance allergic inflammation by a TLR-dependent Th1 immune response.^{26,27} In this context, several recent studies have focused on the ability of LPS to prevent experimental asthma,²⁸ but the molecules and local innate immune cells involved in this modulation have not yet been fully characterized. Therefore, the purpose of the present work was to analyze if protective phenotypes are promoted in CC and AM by an LPS-early stimulation in an ovalbumin (OVA)-induced asthma murine model.

Materials and methods

Animals

This study was performed in female Balb/c mice, which are known to mount strong airways allergic inflammation in experimental asthma model.²⁹ Animals, 5–8 weeks old, were provided by Fun Vet (Universidad Nacional de La Plata, Argentina) and housed under controlled temperature and lighting conditions, with free access to tap water and commercial lab chow (GEPSA FEEDS, Buenos Aires, Argentina). Animals were randomly assigned to four groups ($n=6$ each) and experiments were repeated at least three times.

The animal care and experiments were conducted following the recommendations of the Helsinki convention, and in compliance with local laws on the ethical use of experimental animals.

Experimental design

LPS pre-treatment. On days –3 and –1, the LPS and LPSOVA mice were intranasally exposed to 10 µg of LPS (*Escherichia coli* O55:B5 Sigma-Aldrich; St. Louis, MO, USA) diluted in 50 µL PBS under moderate anesthesia, performed by an intraperitoneal (i.p.) injection of ketamine (10 mg/mL)/xylazine (1 mg/mL) (Alfasan, Woerden, Holland).

OVA sensitization On days 0 and 14, all animals (LPS, LPSOVA, OVA, and control groups) were sensitized by i.p. injections of 0.1 mL of OVA grade VI (1000 µg/mL, Sigma-Aldrich), absorbed to 1 mg of Imject Alum (Pierce Rockford, USA).

OVA challenge. At days 24–33, LPSOVA and OVA mice were challenged daily by an intranasal application of 50 µL of 1% OVA, whereas the control and LPS mice were submitted to intranasal applications of saline (see Figure 1). Then, after 24 h (day 34), mice were sacrificed and processed according to the specific methods outlined further in the text.

The dose of LPS was selected based on a dose–response curve and previous reports determining 10 µg as the less toxic dose that presented suppressive activity on allergic responses.³⁰ The OVA doses for sensitization and challenge treatment was chosen based on our previous studies^{18,19} and other reports.^{31–33}

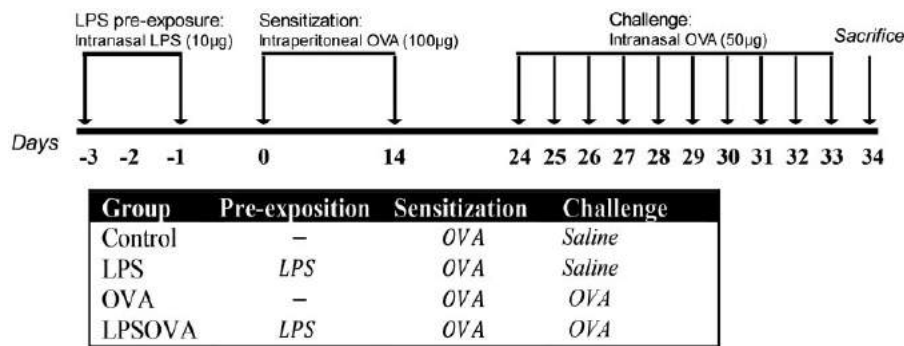


Figure 1 Experimental design and protocols employed in this study. Protocols included experimental groups of Ovalbumin (OVA)-sensitized mice on days 0 and 14, which on days 24 to 33 were then challenged daily with intranasal OVA (OVA group) or sham with saline (control group). Furthermore, two lipopolysaccharide (LPS) pre-exposed groups included mice that received two doses of intranasal LPS and then were either OVA challenged (LPSOVA group) or sham-exposed (LPS group)

Lung histopathology

Right lungs of three mice per group in three experiments were differentially fixed for morphological analysis by intratracheal perfusion as previously described.¹⁸ Briefly, for ultrastructural analysis, lungs were perfused with a mixture of 1% (v/v) glutaraldehyde and 2% (w/v) formaldehyde in 0.1 M cacodylate buffer before being removed and post-treated with 1% osmium tetroxide and embedded in Araldite. Terminal bronchioles and alveoli (identified on 70 nm sections) were then cut (JEOL JUM-7 ultramicrotome) and examined (Zeiss LEO 906 E electron microscope). Meanwhile, histopathological analysis was performed on lungs fixed with 4% formaldehyde, embedded in paraplast, and 5 μ m sections were obtained. For immunostaining or mucous cell staining, slides were dewaxed with xylene, and then rehydrated with a series of decreasing concentrations of ethanol solutions.

Mucous cell staining

Mucous-secreting cells in the bronchiolar epithelium were identified by the Alcian blue-periodic acid Schiff (AB-PAS) staining technique as previously described.¹⁹ Photomicrographs at $\times 400$ were taken using a light microscope (AxioStar Plus, Zeiss, Germany) equipped with a digital camera (AxioCam ERc5s). A total of 15–20 bronchioles (900–1700 μ m diameter) per mouse were analyzed, and the number of AB-PAS positive cells present in epithelia lining per 100 μ m of basement membrane were quantified using Image J Software (NIH version 1.43).

Immunohistochemical analysis of lung tissue

Immunohistochemical staining was performed as described elsewhere.¹⁹ Briefly, after being blocked, the sections were incubated overnight at 4°C with antibodies recognizing SP-D (1:1000 – Chemicon, Temecula, CA, USA), TNF α (1:50 – Hycult, Plymouth Meeting, USA), CCSP (CC10 antibody 1:1000 – Santa Cruz Biotechnology, Santa Cruz, CA, USA), TLR4 (1:100 – Santa Cruz Biotechnology) or EGFR (1:50 – Santa Cruz Biotechnology), with bound antibodies being detected using anti-rabbit (for SP-D, TNF α and CCSP) or anti-goat (for TLR4 and EGFR) biotin-labeled antibodies

(Vector Laboratories, Burlingame, CA, USA) in 1% PBS-BSA. The sections were then incubated with ABC complex (VECTASTAIN Vector Labs, Southfield, MI, USA). Diaminobenzidine (DAB, Sigma-Aldrich), which was used as a chromogen substrate, and the bronchioles (900–1700 μ m diameter) were analyzed and photomicrographs $\times 400$ were taken.

Immunoelectron microscopy

For the ultrastructural detection of CCSP, immunogold labeling was performed as described previously.¹⁸ Embedded (LR White) sections (60 nm) on nickel grids were subsequently incubated with anti-CC10 1:100 (Santa Cruz Biotechnology) overnight followed by the application of an anti-rabbit gold complex 1:20 (Electron Microscopy Sciences, Hatfield, PA, USA).

BAL collection and cell counting

BAL ($n = 9$ mice/group in three different experiment) were obtained as described elsewhere.¹⁸ Briefly, after three serial intra-tracheal instillations of 1 mL PBS, the cells obtained were centrifuged at 200 g, and the supernatant was stored at -70°C for ELISA and Western blot. All cells in pellets were resuspended and counted, with about 12.5×10^4 cells being cytocentrifuged onto the slide and stained with May Grünwald-Giemsa (Biopur Diagnostic, Rosario, Argentina). Cell populations were evaluated for two samples per mouse, and a total of 2400 cells per group were counted.

Alveolar macrophage enrichment and preparation

Alveolar macrophages were isolated (nearly 90%) from BAL and cultivated according to Zhang et al. with modifications.³⁴ For this purpose, all cells in the pellet were resuspended in complete RPMI 1640 supplemented with 10% FCS, 2- β -mercaptoethanol (50 μ M), L-glutamine (2 mM), sodium pyruvate (1 μ M), HEPES (10 mM), penicillin (100 U/mL) and streptomycin (100 μ g/mL) (Sigma) and adjusted to 1×10^6 cell/mL. Macrophages were allowed to adhere at 37°C for 3 h, after which the unattached cells were removed by gently washing with warm PBS.

For immunofluorescence, 3×10^5 cells per well were seeded on glass coverslides (13 mm) on 24-well culture plates. Meanwhile, for arginase activity and NO assay, 6×10^4 cells/well were plated on 96-well culture plates. To determine the nitrites, culture media of 96-well plates were collected and centrifuged for 5 min at 200 g and stored at -20°C until use.

Immunofluorescence

Coverslides (3 per mice) with attached alveolar macrophages obtained from the BAL (three mice per group) were fixed with 4% formaldehyde, permeabilized with 0.25% Triton X-100 in PBS and incubated for 1 h in 5% PBS-BSA to block non-specific binding. Slides were double immunostained by incubating overnight at 4°C with anti-CD68 conjugated with Alexa Fluor 488 (BioLegend, San Diego, CA, USA), to identify the alveolar macrophages, which was followed by an incubation with: rabbit anti-iNOS/NOS Type II 1/60 (BD Biosciences, Franklin Lakes, NJ, USA), mouse anti-arginase I 1/250 (BD Biosciences), goat anti-TLR4 1/400 (Santa Cruz Biotechnology) or rabbit anti-TNF α 1/100 (Hycult). Afterwards, bounding antibodies were detected with Alexa 594 anti-mouse, Alexa 594 anti-goat or Alexa 594 anti-rabbit conjugated secondary antibodies (1/1000 Invitrogen, Frederick, MD, USA). The cells were viewed with fluorescence microscope Axiovert 135 (Zeiss), and serial x60 microphotographs (20 per coverslide) were collected, with all double immunostained cells (1800 per group) being evaluated in three different experiments and the relative percentages were calculated.

Arginase enzyme activity and NO production

Arginase activity was measured in lysates from attached alveolar macrophages as previously described by Corraliza et al with modifications.³⁵ Briefly, cells were lysed with 0.1% Triton X-100 plus protease inhibitors for 30 min. Equal volumes of Tris-HCl (25 mM)-MnCl₂ (10 mM) buffer and lysate were mixed, and the enzyme was activated by heating for 10 min at 55°C . Arginine hydrolysis was performed by incubating the cell lysates with L-arginine (pH 9.7) at 37°C for 60 min and the reaction was stopped upon the addition of 200 μL of $\text{H}_2\text{SO}_4/\text{H}_3\text{PO}_4/\text{H}_2\text{O}$ (1:3:7, v/v/v). The urea concentration was measured at 540 nm after the addition of 25 μL of ISPF (dissolved in 100% ethanol), followed by heating at 100°C for 40 min. The values obtained (expressed as units of activity) were normalized against total protein (U arginase/mg protein) content in adherent cells with one unit of enzyme activity being defined as the amount of enzyme that catalyzed the formation of 1 μmol of urea/min.

NO production was determined in the supernatants of the culture media obtained during the alveolar macrophage purification step using Griess reagent (Britania, Buenos Aires, Argentina). Briefly, 100 μL of culture supernatant was reacted with 200 μL of reagent (1% sulphanilamide/0.1% naphthylethylene diamine dihydrochloride/2.5% H_3PO_4) at room temperature for 10 min, after which the absorbance at 540 nm was determined.

Immunoblotting

By Western blot Muc5ac levels were determined in BAL supernatant, while SP-D, EGFR, and HIF-1 α expressions were evaluated in total lung homogenates from three animals per group in three different experiments as was described.¹⁸ Briefly, after proteins were measured with a Bio-Rad kit (Bio-Rad Laboratories, Hercules, CA, USA), the denatured protein samples were separated on 12% SDS-PAGE and blotted onto a Hybond-C membrane (Amersham Pharmacia-GE, Piscataway, NJ, USA). Membranes were then blocked with 5% defatted dry milk in PBS/0.1% Tween 20 and incubated for 3 h with one of the following antibodies: rabbit anti-SP-D (1:1000 – Chemicon, Temecula, CA, USA), goat anti-EGFR (1:200 – Santa Cruz Biotechnology), rabbit anti-HIF-1 α (1:1500 – Novus Biologicals, Littleton, CO, USA), or mouse anti-Muc5ac (1:200 – Abcam, Maryland, USA). Blots were incubated with a peroxidase-conjugated (HRP) anti-rabbit (Jackson ImmunoResearch Labs Inc, West Grove, PA, USA), anti-goat (sc-2352, Santa Cruz Biotechnology), or anti-mouse (Jackson ImmunoResearch) secondary antibodies at a 1:2000 dilution. Finally, the membranes were rinsed in PBS/0.1% Tween-20 and exposed to SuperSignal West Pico Chemiluminescent Substrate (Thermochemical, Rockford, IL, USA) following the manufacturer's instructions. Emitted light was captured on Hyperfilm (Amersham-Pharmacia) and a densitometry analysis was performed by applying the Scion Image software (V. beta 4.0.2, Scion Image Corp., Frederick, MD, USA). For lung homogenates, the expression of ACTB (1: 5:000; monoclonal anti- β -actin; Sigma-Aldrich) was used as an internal control to confirm equivalent total protein loading.

Dot blot analysis

The CCSP protein expression was evaluated in lung homogenates after total protein measurement was performed using a Bio-Rad kit. Samples were then adjusted to 5 $\mu\text{g}/\mu\text{L}$ in PBS, pH 7.4, and 5 μL of each sample were spotted onto a Hybond-C membrane (Amersham Pharmacia). Then the membrane was blocked with 5% fat-free milk in PBS buffer for 1 h and incubated for 3 h with a rabbit primary antibody anti-CC10 1:500 (Santa Cruz Biotechnology) in blocking buffer at room temperature. After washing with PBS-Tween-20 buffer, the membrane was treated with a HRP-conjugated anti-rabbit antibody (Jackson ImmunoResearch) and the next handle was as described above for Western blot.

Cytokine detection by ELISA

Cytokines production was measured in BAL by applying commercially available sandwich ELISA kits for: IL-4, IFN γ (BD Biosciences), TNF α (eBioscience, San Diego, CA, USA), TSLP and IL-12 (p70) (Biolegend, San Diego, CA, USA), and IgE and IgG1 (eBioscience) following the manufacturer's instructions.

Measurement of airway responsiveness

In vivo airway hyperresponsiveness (AHR) was measured 24 h after OVA challenge in response to increasing doses of methacholine by invasive plethysmography.

Six to eight mice per group were tracheostomized and intubated to a small animal ventilator (FinePointe Series RC Sites, Buxco Research System, Wilmington, DE, USA). Then, the dynamic airway pressure was measured for 3 min and the maximal resistance measurement was obtained both before and after increased doses of aerosolized methacholine (0.0–30 mg/mL).

Statistical analysis

Data obtained were analyzed by one-way ANOVA, followed by post hoc comparison with the Tukey–Kramer test. A $P < 0.05$ significance level was used for all tests.

Results

LPS modulated the OVA-induced allergic airways inflammation

We first evaluated, in a separate group of animals, the inflammatory cell profile and the histologic injury of the lungs that a dose of 10 μ g of LPS represents. To this aim, we quantified neutrophils recruitment in BAL and found that their percentage increased significantly at 4–8 h post-instillation and at 24 h were normalized, while TNF α levels followed a similar kinetic with maxim values at 4 h and a normalization at 24 h (Supplementary Figure 1 available online). The morphological analysis also evidenced an active response of CC that showed marked hypertrophy and dilated rough endoplasmic reticulum cisternae at

4–8 h, with a reversion of these parameters at 24 h. These cells also overexpressed anti-inflammatory CCSP and anti-bacterial SP-D during this time (not shown).

Then, we evaluated the impact of LPS pre-treatment on the characteristic inflammatory microenvironment of asthma; the inflammatory cells and cytokine secretion were analyzed in BAL. In the LPSOVA group, a reduced number of inflammatory cells were obtained from BAL compared to OVA ($P < 0.001$), mainly due to a marked diminution in the number of eosinophils ($P < 0.001$); meanwhile, macrophages and lymphocytes remained unchanged but neutrophils were increased ($P < 0.001$ vs control) (Figure 2a). In addition, a lower level of IL-4 in LPSOVA was detected compared to the OVA group ($P < 0.01$) (Figure 2d), while the Th1-related cytokines, Interferon- γ (IFN γ) ($P < 0.001$ vs control), IL-12 ($P < 0.05$ vs control) (Figure 2b to c), and Tumor necrosis factor α (TNF α) ($P < 0.001$ vs control) (Figure 3d) were found to be induced. In the LPS group, neither BAL cells analysis nor cytokines content were different from control. We finally evaluated IgE and IgG1 and found that the allergen-induced increase of IgE production was avoided in LPSOVA while only a slight increase of IgG1 ($P < 0.05$ vs control) was observed (Figure 2e).

To test whether the inflammatory parameters were accompanied by changes in lung functionality, AHR was measured in mice. As expected, AHR was enhanced in the OVA group compared to control and LPS ($P < 0.01$), while LPSOVA exhibited lower levels than OVA. However, a complete prevention was not achieved, with AHR remaining elevated in LPSOVA compared to control ($P < 0.05$) (Figure 2f).

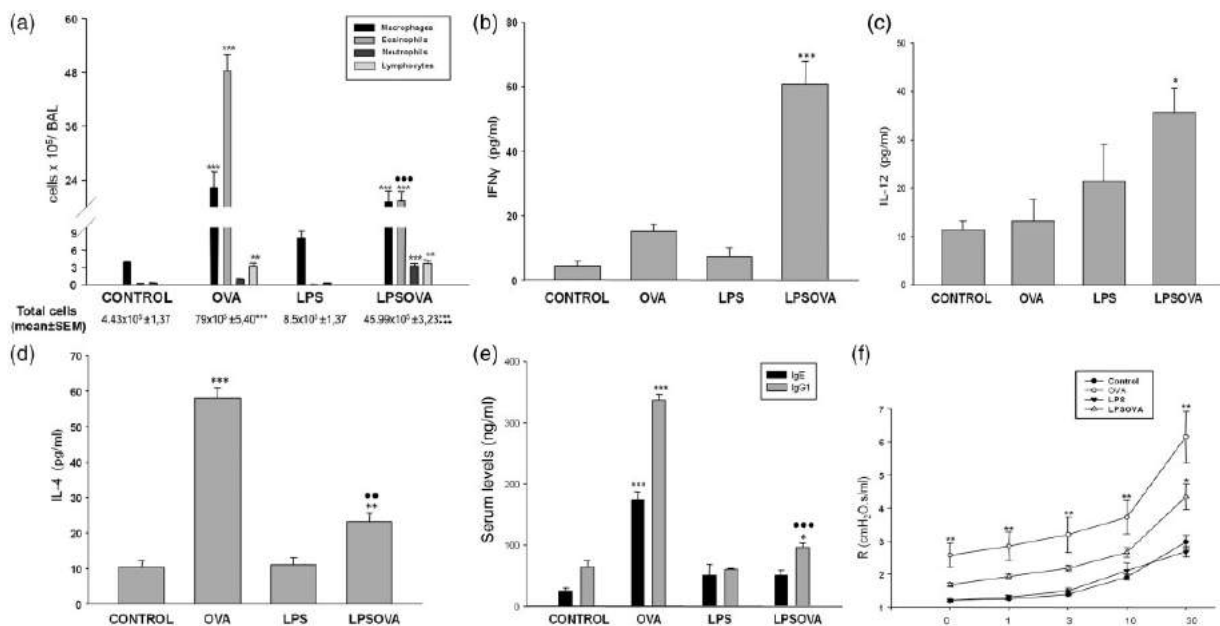


Figure 2 Inflammatory microenvironmental state. (a) Differential quantification of cell populations in bronchoalveolar lavage (BAL). Bar graph represents total number of macrophages, eosinophils, neutrophils, and lymphocytes in BAL. (b), (c) and (d): Levels of IFN γ , IL-12(p70), and IL-4 in BAL by ELISA. (e) IgE and IgG1 levels by ELISA in mice serum. (f) Measurement of airway reactivity in response to increasing doses of methacholine (Mch) analyzed by invasive plethysmography. Graph represents the resistance measurements obtained 24 h after last intranasal challenge from at least eight animals per group in two independent experiments. Data represent mean \pm SD *** $P < 0.001$ vs control, ** $P < 0.01$ vs control, * $P < 0.05$ vs control, ● $P < 0.01$ vs OVA, ●● $P < 0.001$ vs OVA

LPS promoted innate immunity markers on CC and AM which were maintained after allergen challenge

In control, CC displayed no TLR4 or TNFα immunoreactivity (Figure 3a), whereas a weak basal TNFα expression was observed in the subepithelial stromal cells. In the OVA group, although bronchiolar epithelium was also negative for both molecules, the subepithelial TNFα expression was highly increased, probably due to stromal hypertrophy (asterisk in Figure 3a). LPS incited a strong TLR4 staining on CC, which was seen in both LPS and LPSOVA mice, while TNFα was only expressed in CC of the LPSOVA group (arrows in Figure 3a).

Considering that AM represents a main player of the lung innate immunity, the expression of TLR4 and TNFα was assessed by immunofluorescence in these cells *ex vivo* (Figure 3b). The analysis of TLR4 and TNFα displayed a similar expression pattern as that described for CC, with

an equally intense signal occurring in the LPS and LPSOVA groups ($P < 0.001$ vs control), but which was very low in OVA. Moreover, the percentage of CD68+/TNFα+ cells was reduced in OVA group compared to control ($P < 0.05$) (Figure 3c).

It is noteworthy that even though LPSOVA and LPS groups had similar percentages of TNFα positive AM, this cytokine was only increased in BAL from LPSOVA (Figure 3d), probably due to the contribution of CC secretion and to the higher number of AM observed in this group ($P < 0.001$) (Figure 2a).

Asthma-induced CC mucous metaplasia and TSLP expression was modulated by LPS pre-exposition

As previously described,¹⁸ the OVA challenge incited mucous cell metaplasia in the lung bronchioles (Figure 4a), which was corroborated by an increased

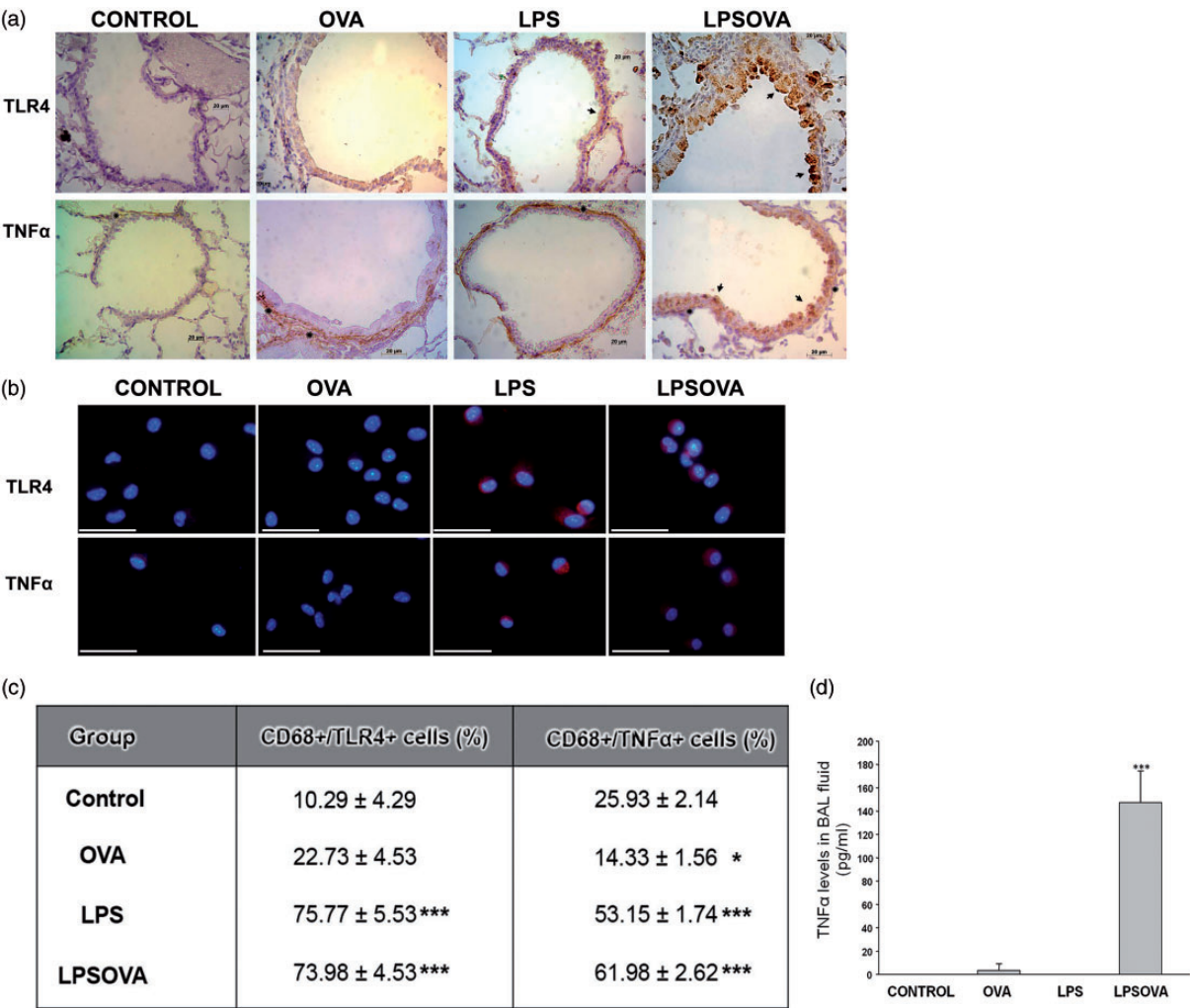


Figure 3 Analysis of TLR4 and TNFα expression in club cells and alveolar macrophages. (a) Representative micrographs of TLR4 and TNFα immunostaining performed on lung sections. Positive club cells are stained brown with diaminobenzidine (arrow) against the blue hematoxylin counter staining. Asterisks indicate TNFα positive expression in the subepithelial compartment. Scale bars: 20 μm. (b) Immunofluorescence staining for TLR4 or TNFα in cover slides enriched in macrophages obtained by bronchoalveolar lavage; CD68 immunofluorescence was performed to determine the total macrophage number. Representative micrographs show overlays of cell nuclei staining for DAPI and red TLR4 or TNFα fluorescence, while the percentage of CD68+/TLR4+ cells and CD68+/TNFα+ cells is shown in (c). (d) Levels of TNFα in bronchoalveolar lavage (BAL) fluid determined by ELISA. Data are represented as mean ± SEM. *** $P < 0.001$ vs control, * $P < 0.05$ vs control. (A color version of this figure is available in the online journal.)

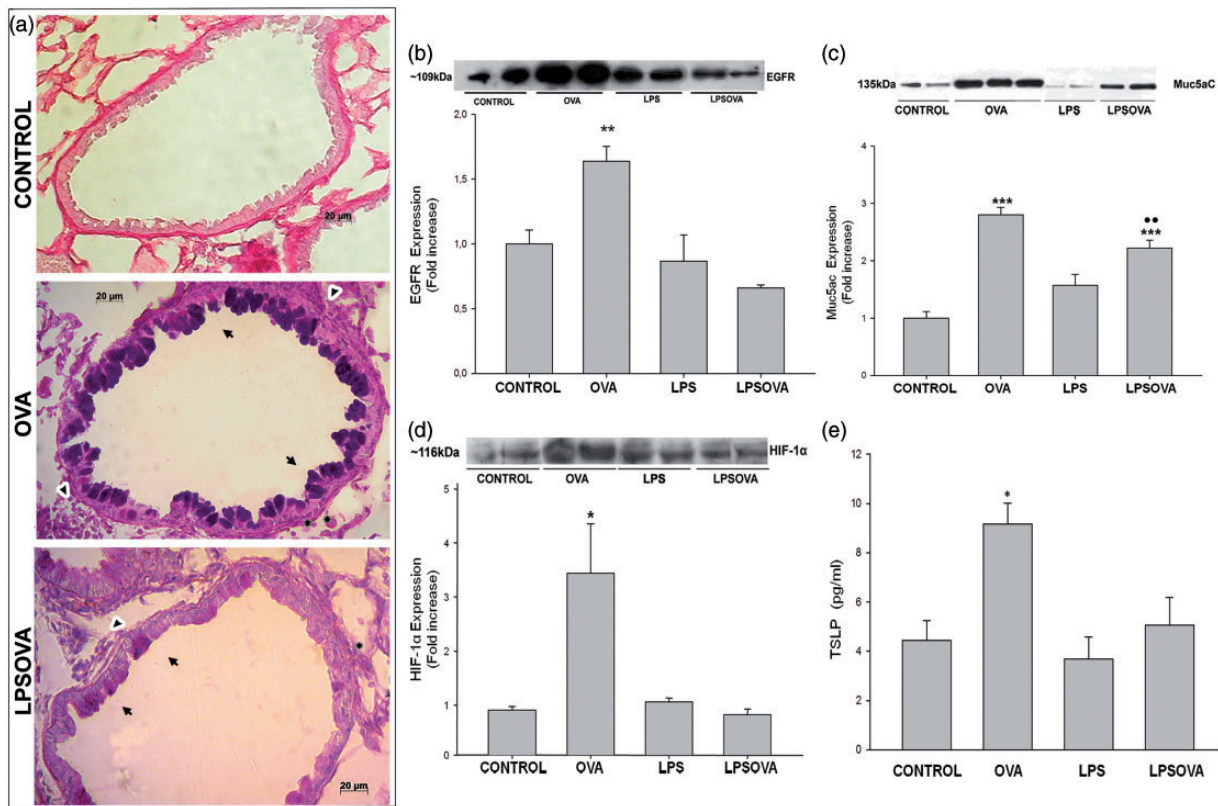


Figure 4 Mucous metaplasia analysis. (a) Representative photomicrographs of Alcian blue-periodic acid Schiff (AB-PAS) staining on lung sections from control, OVA, and LPSOVA mice. Arrows indicate AB-PAS positive cells in OVA and LPSOVA groups, while asterisks point out the enlarged subepithelial compartment due to thickening of the smooth-muscle cell layer and PAS positive collagen deposition at the basement membrane. In addition, arrowheads in OVA and LPSOVA mice indicate infiltrating inflammatory cells. Scale bars: 20 μm. (b) Western blot of Epithelial Growth Factor Receptor (EGFR). Graph represents fold increase of the relative EGFR/β-actin expression in lung homogenate by densitometric analysis. (c) Western blot of Muc5ac. Graph represents fold increase of the relative Muc5ac expression by densitometric analysis in bronchoalveolar lavage. (d) Western blot of Hypoxia inducible factor 1α (HIF-1α). Graph represents fold increase of the relative HIF-1α/β-actin expression in lung homogenate by densitometric analysis. In (b)–(d), underlined blots indicate independent samples of each group. (e) Level of TSLP in BAL analyzed by ELISA. Data are represented as mean ± SEM, * $P < 0.05$ vs control, ** $P < 0.01$ vs CONTROL, *** $P < 0.001$ vs control, ●● $P < 0.01$ vs OVA. (A color version of this figure is available in the online journal.)

number of AB-PAS-positive cells in the bronchiolar epithelium compared with OVA (11.4 ± 0.54 vs 0.2 ± 0.61 , $P < 0.001$), the enlarged subepithelial stroma (arrowhead in Figure 4a) and by the overexpression of EGFR ($P < 0.01$) as well as Muc5ac ($P < 0.001$) compared to control (Figure 4(b) and (c)). Furthermore, we also evaluated the Hypoxia-inducible factor 1 (HIF-1) expression. HIF-1 is a transcription factor downstream EGFR signaling that exerts a positive control in the regulation of Muc5ac in allergic mucous metaplasia,¹⁷ and we found that HIF-1 subunit α increased significantly in OVA mice ($P < 0.05$) (Figure 4d).

We next evaluated the expression of TSLP, an epithelial cell-derived cytokine that increases during the allergen exposition and is important in initiating the Th2-biased response by dendritic.³⁶ As expected, we found significantly higher levels of TSLP in OVA group ($P < 0.05$ vs control) (Figure 4e). Meanwhile, the previous instillation of LPS (LPSOVA group) abrogated OVA-induced increment of EGFR, HIF-1α and TSLP levels which were maintained as in control (Figure 4(b), (d) and (e) respectively). Moreover, only in OVA mice a strong positive expression in CC-apical cytoplasm was revealed in the EGFR immunohistochemical analysis (see Supplementary

Figure 2 available online). Even though in LPSOVA lower AB-PAS positive cells were found (3.07 ± 0.39 vs 11.4 ± 0.54 , $P < 0.001$) and Muc5ac levels decreased significantly ($P < 0.001$) in contrast to OVA (Figure 4c), these parameters continue higher ($P < 0.01$) than control (AB-PAS+ cells: 3.07 ± 0.39 vs 0.2 ± 0.61). The basal levels of all these parameters were shown in animals that received only LPS.

LPS contributed to preserve CC normal phenotype and their defensive molecules content

At the ultrastructural level, control mice showed a typical CC profile, characterized by the presence of a dome-shaped cupola, a nucleus in the basal position, numerous polymorphic mitochondria and a rough endoplasmic reticulum (RER) in the cytoplasm, along with a few plasma membrane-bound spherical electron-dense secretory granules (Figure 5a). In the LPS group, the main change in CC was an important increase in electron-dense secretory granules, compared with control (Figure 5c). In agreement with our previous results,¹⁸ CC experienced mucous cell metaplasia after allergic inflammation (Figure 5b), which was corroborated by a

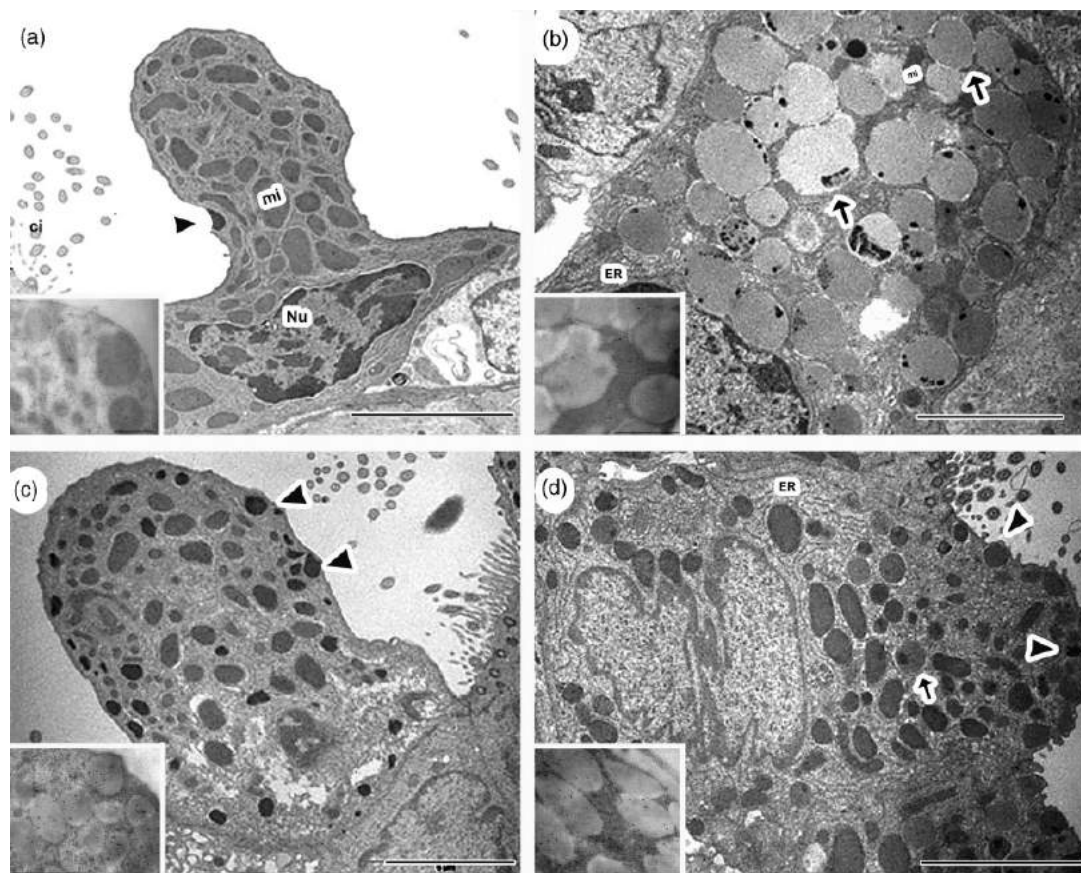


Figure 5 Club cell ultrastructural analysis. Representative electron micrograph images of club cell morphology of control (a), OVA (b), LPS (c), and LPSOVA groups (d) are shown. Scale bar represents 5 μ m. Inset electron micrographs in (a)–(d) show CC16 immunogold labeling of secretory granules for the different groups. Inset bar represents 2 μ m. mi: mitochondria, Nu: nucleus; ER: endoplasmic reticulum; arrowheads: normal electron dense granules; arrows: electron lucid granules

hypertrophied cytoplasm filled up with numerous large electron-lucent secretory granules containing scarce CCSP expression (inset Figure 5b), slim mitochondria and abundant RER; ciliated cells presented neither ultrastructure nor number significant changes. In contrast, most CC of the LPSOVA group displayed a more typical profile (Figure 5d) with the electron-dense secretory granules having a high expression of CCSP (inset Figure 5d). However, the presence of well-developed RER and some electron-lucent granules was also observed.

OVA-allergic inflammation also led to a weak expression of CCSP and SP-D when compared with control group (Figure 6a), whereas for both LPS and LPSOVA groups, a strong immunoreactivity of CCSP and SP-D was observed (Figure 6a). Dot blot assay evidenced that LPS-instillation increased CCSP content in LPS group and contributed to maintain basal levels in LPSOVA (Figure 6b), suggesting a specific LPS-induced response of CC that elevated the defense molecules and seemed to be preserved in spite of allergen stimulus. The total SP-D lung content in LPSOVA indicated a partial prevention of SP-D reduction (Figure 6c), contrasting with the *in situ* immunohistochemical analysis (Figure 6a). This may be explained by the fact that SP-D is not only produced by CC but also by Type II alveolar cells.

LPS avoided OVA-induced changes in AM and promoted features of CAM phenotype

The polarization state of alveolar AM was evaluated by the immunofluorescence expression of iNOs (CAM phenotype) or Arginase1 (Arg-1) (AAM phenotype), following the adhesion step (Figure 7a), which isolated nearly 90% of CD68 positive macrophages.

The analysis of the percentage of CD68/iNOs and CD68/Arg-1 positive cells (Figure 7b) revealed very few CD68+ alveolar macrophages that expressed Arg-1 or iNOs in control or the LPS group. However, in the OVA group, the allergic microenvironment induced a strong Arg-1 expression in most of the CD68+ macrophages, while the iNOs expression was similar to control (Figure 7(a) and (b)). In contrast, in the LPSOVA group, the macrophages expressing Arg-1 were fewer than in OVA, with the LPS-induced iNOs+ macrophages prevailing (Figure 7(a) and (b)). Furthermore, the enzyme functional assays corroborated these results, indicating a high arginase activity (typical of AAM macrophages) in the OVA group versus control (Figure 7c) and a significant production of NO in the alveolar macrophages from LPSOVA mice (Figure 7d).

Using light microscopy, AM from the OVA group demonstrated morphological changes in the cytoplasm, as they appeared enlarged, highly vacuolated, and often

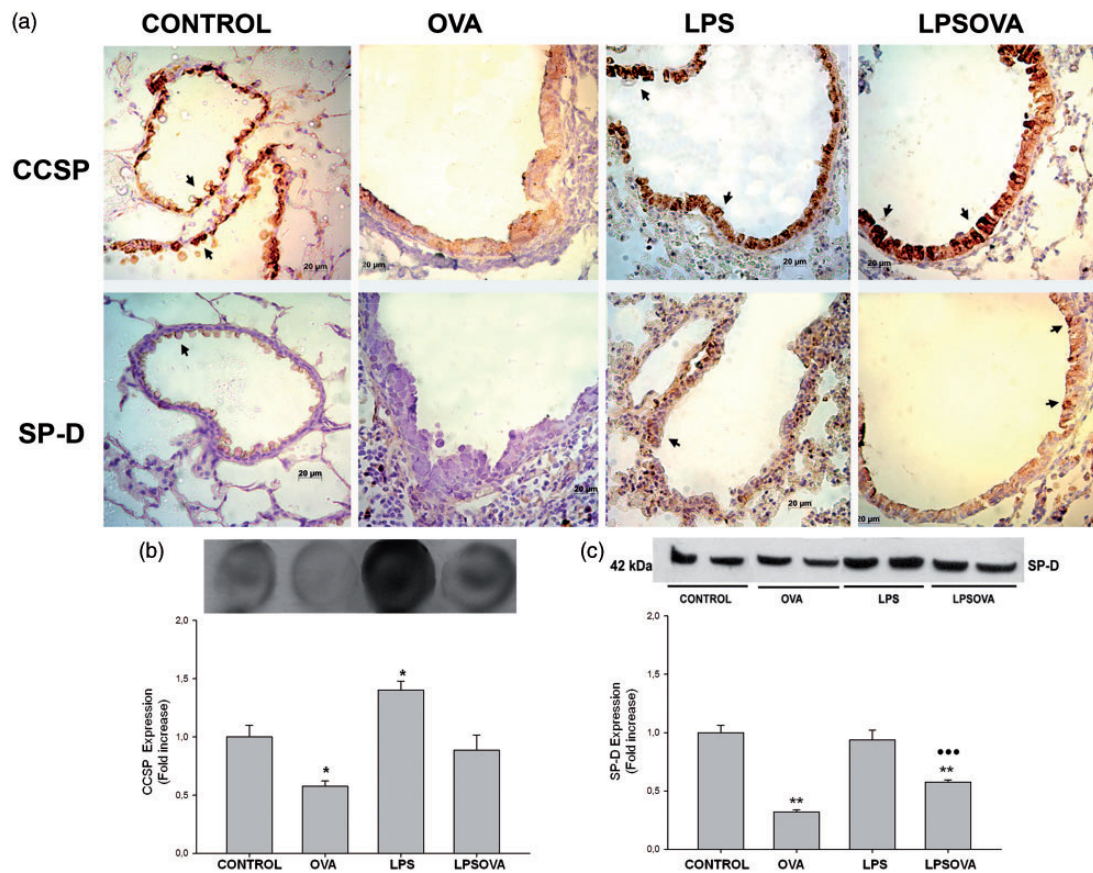


Figure 6 Analysis of Club cell secretory protein (CCSP) and surfactant (SP)-D content. (a) CCSP and SP-D immunostaining performed on lung section of all groups. Positive club cells appear in brown (arrows) against the blue counter stain of haematoxylin. Scale bars: 20 µm. (b) Dot blot of CCSP in lung homogenates. Graph represents fold increase of the relative CCSP expression in lung homogenate by densitometric analysis. (c) Western blot of SP-D lung content. Graph represents fold increase of the relative SP-D/β-actin expression in lung homogenate by densitometric analysis. Underlined blots indicate independent samples of each group. Data are represented as mean ± SEM, * $p < 0.05$ vs Control, ** $p < 0.01$ vs control, *** $p < 0.001$ vs OVA. (A color version of this figure is available in the online journal.)

multinucleated (see Supplementary Figure 3 available online). Moreover, histological examination revealed PAS positive material in these multinucleated giant cells (see Supplementary Figure 4 available online). At the ultrastructural level, the allergic inflammation incited drastic changes in the AM, which appeared in the OVA group as large polyhedral cells with eccentric nuclei and an enlarged cytoplasm with numerous phagosomes (Figure 8c). This differed from control and LPS mice, where macrophages appeared as elongated cells with a central nucleus and a cytoplasm with scarce phagosomes (Figure 8a). Furthermore, while slim cytoplasmic filopodia-like projections appeared in control (inset Figure 8a), the cell surface of AM showed thick cytoplasmic projections (inset Figure 8c) in OVA mice. In contrast, macrophages from the LPSOVA group preserved and expanded the filipodial projections at the cell surface, with more pronounced RER and Golgi cisterns being exhibited as well as numerous secretory granules (Figure 8(d) and inset).

Discussion

Epithelial CC and AM maintain lung homeostasis against inhaled injuries at the bronchioalveolar level, which is a

key site for asthma pathogenesis. In the present work, we reported that the exposition to LPS previous to the allergen challenge contributed to sustaining the typical phenotype of CC, which was rich in immunomodulatory and anti-allergic products, and promoted a phenotype of CAM on AM. This was concurrent with a reduction of allergy-associated parameters, including TSLP expression, Th2 cytokines, eosinophil influx, and airway hyperresponsiveness. Thus LPS pre-exposition changed the local microenvironment in response to allergen stimulus with the induction of anti-allergic proteins and host defense mediators in CC and AAM followed by Th1-related cytokine, while the airway remodeling process along with the chemokines and Th2-related cytokines was reduced.

Allergen stimulation of protease-activated receptor 2 (PAR2), C-type lectin receptors, or TLRs triggers the production TSLP, IL-25, and IL-33 cytokines by airway epithelial cells.³⁷ TSLP has been identified as a “master switch” for allergic inflammation, by activating airway dendritic cells and by increasing the number of Th2 cells and their cytokines.⁸ The attenuation of OVA-induced TSLP by LPS pre-treatment is a novel finding

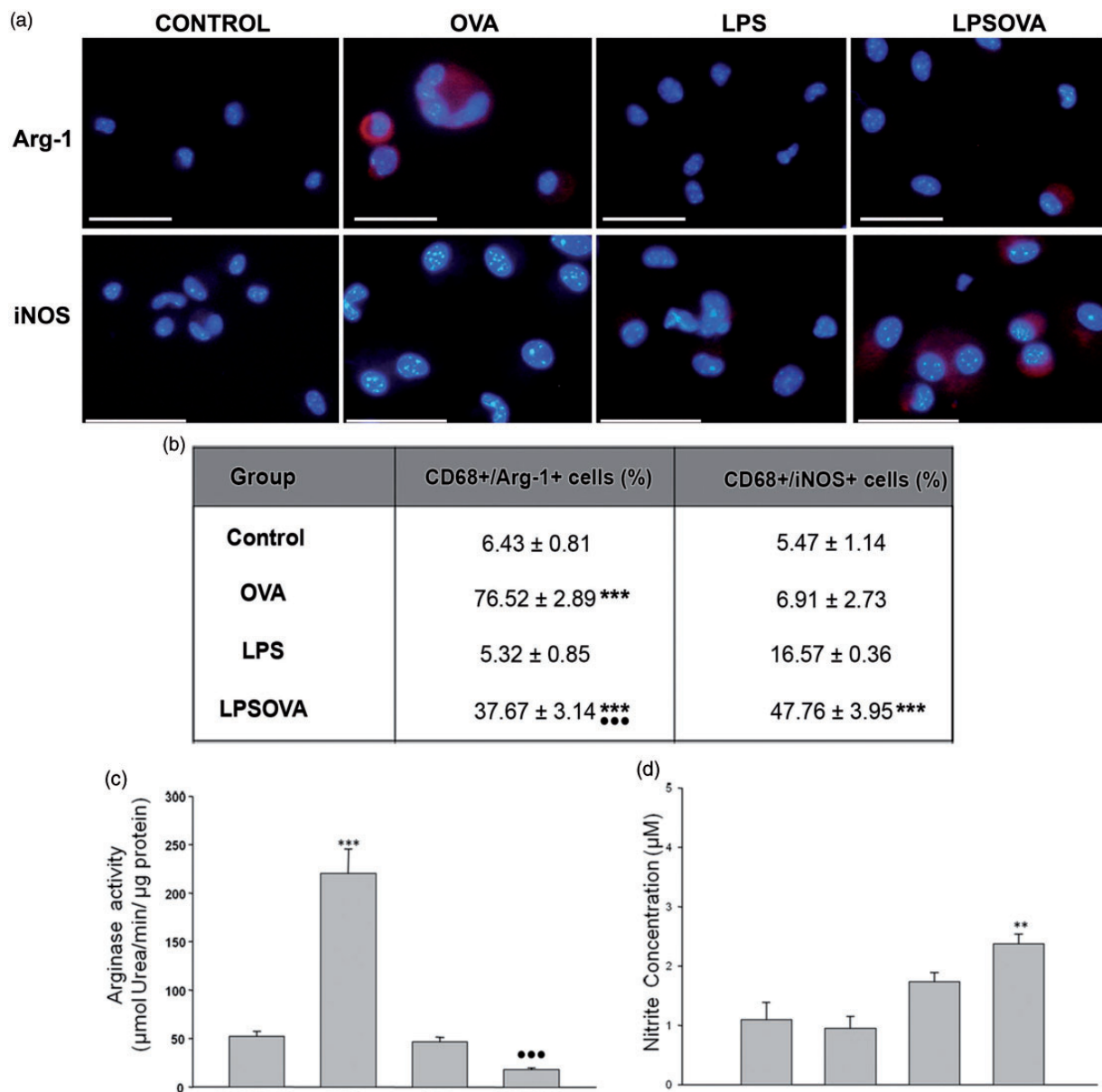


Figure 7 Analysis of the macrophage polarization biomarkers Arg-1 and iNOS enzymes in alveolar macrophages. (a) Immunofluorescence of CD68 together with arginase-1 (Arg-1) or inducible NO synthase (iNOS) was realized in cover slides enriched in macrophages obtained by bronchoalveolar lavage (BAL); CD68 co-localization was performed to determine the total macrophage number. Representative micrographs show overlays of cell nuclei staining for DAPI and red Arg-1 or iNOS fluorescence only, while the counting percentage of double labeled CD68+/Arg-1+ cells and CD68+/iNOS+ cells are shown in (b). (c) Arginase activity assay performed on homogenates of alveolar macrophages purified from BAL. Graph represents units of arginase activity, defined as the amount of enzyme that catalyzed the formation of 1 μmol urea/min, normalized against total protein. (d) Nitrite levels detected by Griess reaction in culture media obtained during alveolar macrophage purification step. Data are represented as mean \pm SEM, scale bars: 20 μm , *** P < 0.001 vs control, ** P < 0.01 vs control, ●●● P < 0.001 vs OVA. Scale bars: 20 μm . (A color version of this figure is available in the online journal.)

tightly associated with the marked reduction of allergic parameters, although additional studies *in vitro* will be necessary to determine the LPS-induced mediator implicated in this TSLP modulation.

On the other hand, the preservation of the CC biological activities with a key role in both lung host defense and in allergic processes^{11,13,16} was an important contribution of the early activation of innate mechanisms. Previous findings of our group revealed an alteration of the CC defensive mechanisms, including the CCSP and

SP-D content, along with the mucus metaplasia establishment.^{18,19} In this study, LPS exposition prior to allergen challenge resulted in a meaningful reduction in the mucus hypersecretion, which correlated with decreased EGFR expression. Indeed, CC achieved a better preservation of their typical phenotype, including CCSP and SP-D content together with the increase in TLR4 and TNF α expression. In correlation, in LPS group CC exhibited increased CCSP and TLR4 content, indicating that endotoxin induces a priming state that was preserved despite of the

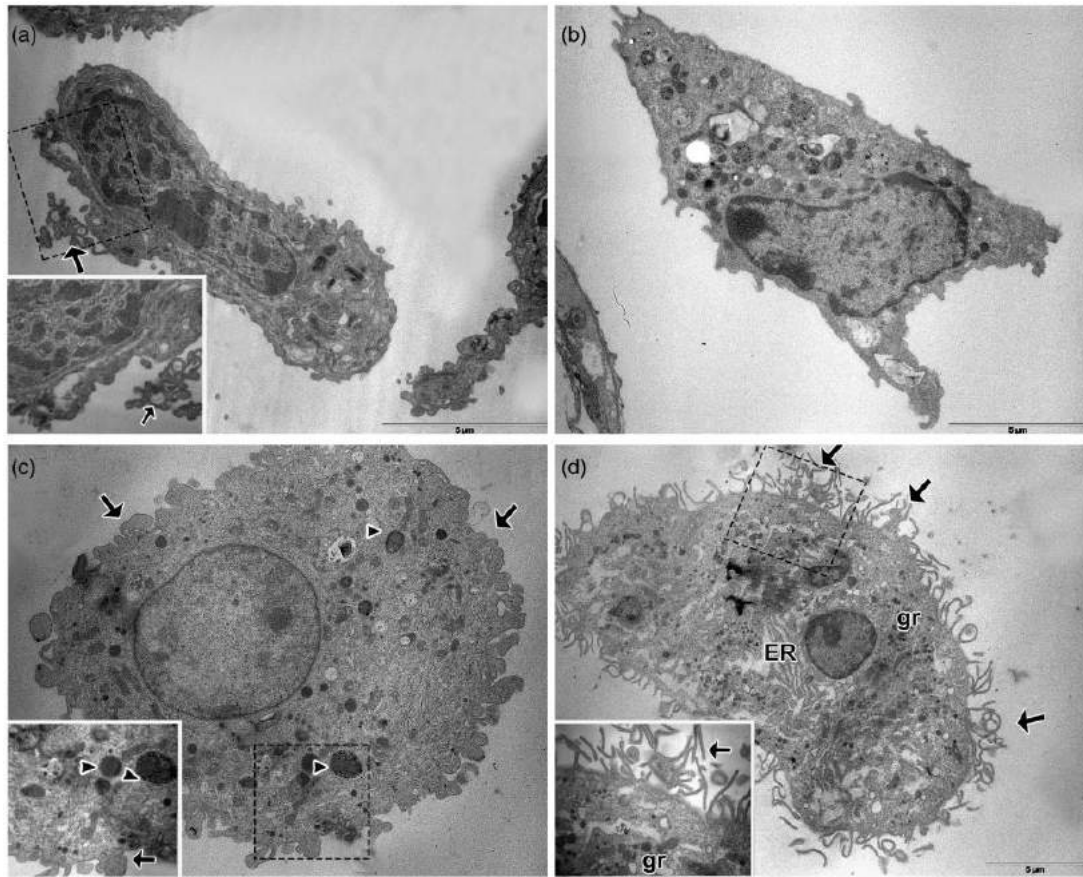


Figure 8 Alveolar Macrophage ultrastructural analysis. Representative electron micrographs illustrate the morphology of the alveolar macrophages (AM) in lung serial sections of control (a), LPS (b), OVA (c), and LPSOVA groups (d). Scale bar represents 5 µm. Boxed area in panels (a), (c), and (d) is enlarged and shown as an inset to reveal details of the AM morphology. Arrows indicate filopodial projections and arrowheads show phagosomes. ER: endoplasmic reticulum; gr: granules

subsequent allergen challenge. Although CC response to LPS has been described before,³⁸ here we report for the first time a possible interrelation between this response and asthma. However, further experiments *in vitro* using gain/loss-of-function transgenic animals are critical for gaining a better understanding of the importance of CCSP and SP-D in LPS-protective mechanisms.

We also evaluated the response of alveolar macrophages which are professional innate immune cells in lung.⁴ During allergic inflammation, AM become AAM,²² a phenotype also known as M2-macrophage, which is strongly associated to airway remodeling and the exacerbation of asthmatic parameters. In agreement, in the present work, OVA induced morphological and functional features compatible with AAM on AM. The enlargement of AM and abundant heterogeneous engulfed material seen at the ultrastructural level and the PAS positive content is indicative of a high extracellular matrix turnover, a property previously described to AAM.^{4,7} In contrast, when asthma was developed after the LPS pre-treatment, AM exhibited TLR4 expression and the production of TNF α and NO, which are pro-inflammatory characteristics compatible with a CAM profile that contribute to suppress allergic airway

inflammation.^{21,39} The increase in secretory granules and filopodial projections observed in CAM by electron microscopy may contribute to a better microbial phagocytosis and cytokine secretion, as has been recently postulated.⁴⁰ This constitutes probably the first characterization of AM in a combined Th1/Th2 micro-environment by electron microscopy, with specific morphological features of macrophage polarization being revealed in AAM as well as in CAM.

The protective effects of endotoxins, by activating innate immunity and effector Th1 immune responses on allergy, constitute the main evidence for the hygiene hypothesis. However, several reports have argued against this concept, linking endotoxins and TLR signaling with asthma exacerbations.^{41,42} In most of these works, and in contrast with our model, LPS was applied at lower doses as an adjuvant for antigen sensitization.^{31,41,42} Hammad et al. induced allergy with HDM extract containing a sub-nanogram range of endotoxin contamination to demonstrate that TLR4 triggering on structural cells causes production of the innate pro-allergic cytokines (TSLP, IL-25, IL-33) and that the absence of TLR4 on structural cells, but not on hematopoietic cells, abolishes HDM-driven allergic airway inflammation. Also Nigo et al. used an

experimental asthma model with a low-dose LPS administration in order to demonstrate that mast cells play a crucial role for LPS-mediated enhancement of eosinophilic airway inflammation. Nevertheless, our results are in agreement with the hygiene hypothesis, as they reveal a high dose LPS-induced protective effect against asthma, even though a complete prevention of allergic parameters (i.e. AHR) was not achieved as described elsewhere.^{43,44} In those studies, LPS was applied during the gestational/neonatal lapse, which is considered nowadays as a better window of opportunity for triggering an appropriate maturation of innate immunity.⁴⁵

An interesting finding of this study was the enhancement in CC host defense proteins with anti-allergic properties that persisted after an allergen challenge. A growing body of evidence suggests that repeated microbial exposure produces a long-term boost of innate cell functions,⁴⁶ which may positively modulate secondary unrelated injuries such as allergic diseases. Even though we could not discern if the persistence in LPS-induced defensive cell phenotype is an epi-phenomenon, our study might be helpful toward achieving allergy inflammation prevention and is in agreement with the view that the airway epithelium is a crucial regulator of inflammation and the remodeling process in asthma.⁴⁷

Taken together, these results indicate that the previous onset of natural airway anti-allergic mechanisms and Th1 mediators counterbalanced proTh2-derived factors as TSLP and attenuated asthma development. Finally, this investigation provides further data for the research for new therapeutic approaches focused on increasing airways' resistance to the inhaled environment rather than suppressing the inflammatory process.

Authors' contributions: LNG carried out the murine studies, the differential cell counts, the immunohistochemical and the immunoblot assay, carried out the ELISA, and drafted the manuscript. CL participated in the isolation and culture of alveolar macrophages as well as in the immunofluorescence and statistical analyses. EMUE participated in the differential cell counts, and in the ensuring that questions related to the accuracy/integrity of the work were appropriately investigated. PLA, JMB and FPP performed and analyze the pulmonary function testing. MSM and CES collaborated in the analysis of macrophage arginase 1 and iNOS and in the critical revision of the manuscript. AAQ and CAM participated in the draft of the manuscript and revising it critically for important intellectual content. CAM performed the ultrastructural analysis, was involved in the conception and design of the study, and coordinated it. All authors read and approved the final manuscript.

ACKNOWLEDGEMENTS

The authors are thankful to Elena Pereyra, Lucía Artino, Soledad Santa Cruz, Cristian Giacomelli and Paula Alejandra Icely for their excellent technical assistance as well as Liliana Sosa for her constant advice. We also thank Dr. Paul Hobson, native speaker, for revision of the manuscript, and the

department's leader Alicia Torres, who provided general support to this work. This work was supported by the Consejo Nacional de Investigaciones Científicas y Tecnológicas (CONICET) [No. 11220100100280] and the Agencia Nacional de Promoción Científica y Tecnológica (ANPCyT) [PICT 2012-0654].

REFERENCES

- Bateman ED, Hurd SS, Barnes PJ, Bousquet J, Drazen JM, FitzGerald M, Gibson P, Ohta K, O'Byrne P, Pedersen SE, Pizzichini E, Sullivan SD, Wenzel SE, Zar HJ. Global strategy for asthma management and prevention: GINA executive summary. *Eur Respir J* 2008;**31**:143–78
- Galli SJ, Tsai M, Piliponsky AM. The development of allergic inflammation. *Nature* 2008;**454**:445–54
- Schleimer RP, Kato A, Kern R, Kuperman D, Avila PC. Epithelium: at the interface of innate and adaptive immune responses. *J Allergy Clin Immunol* 2007;**120**:1279–84
- Murray PJ, Wynn TA. Protective and pathogenic functions of macrophage subsets. *Nat Rev Immunol* 2011;**11**:723–37
- Barnes PJ. Immunology of asthma and chronic obstructive pulmonary disease. *Nat Rev Immunol* 2008;**8**:183–92
- West EE, Kashyap M, Leonard WJ. TSLP: A key regulator of asthma pathogenesis. *Drug Discov Today Dis Mech* 2012;**9**:3–4
- Zhou B, Comeau MR, De Smedt T, Liggitt HD, Dahl ME, Lewis DB, Gyarmati D, Aye T, Campbell DJ, Ziegler SF. Thymic stromal lymphopoietin as a key initiator of allergic airway inflammation in mice. *Nat Immunol* 2005;**6**:1047–53
- Liu YJ, Soumelis V, Watanabe N, Ito T, Wang YH, Malefyt Rde W, Omori M, Zhou B, Ziegler SF. TSLP: an epithelial cell cytokine that regulates T cell differentiation by conditioning dendritic cell maturation. *Annu Rev Immunol* 2007;**25**:193–219
- Holgate ST. The airway epithelium is central to the pathogenesis of asthma. *Allergol Int* 2008;**57**:1–10
- Raoult E, Balloy V, Garcia-Verdugo I, Touqui L, Ramphal R, Chignard M. *Pseudomonas aeruginosa* LPS or flagellin are sufficient to activate TLR-dependent signaling in murine alveolar macrophages and airway epithelial cells. *PLoS ONE* 2009;**4**:e7259
- Reynolds SD, Malkinson AM. Clara cell: progenitor for the bronchiolar epithelium. *Int J Biochem Cell Biol* 2010;**42**:1–4
- Mukherjee AB, Zhang Z, Chilton BS. Uteroglobin: a steroid-inducible immunomodulatory protein that founded the Secretoglobulin superfamily. *Endocr Rev* 2007;**28**:707–25
- Hung CH, Chen LC, Zhang Z, Chowdhury B, Lee WL, Plunkett B, Chen CH, Myers AC, Huang SK. Regulation of TH2 responses by the pulmonary Clara cell secretory 10-kd protein. *J Allergy Clin Immunol* 2004;**114**:664–70
- Hartl D, Griese M. Surfactant protein D in human lung diseases. *Eur J Clin Invest* 2006;**36**:423–35
- Kuperman DA, Huang X, Nguyen L, Holscher C, Brombacher F, Erle DJ. IL-4 receptor signaling in Clara cells is required for allergen-induced mucus production. *J Immunol* 2005;**175**:3746–52
- Sonar SS, Ehmke M, Marsh LM, Dietze J, Dudda JC, Conrad ML, Renz H, Nockher WA. Clara cells drive eosinophil accumulation in allergic asthma. *Eur Respir J* 2012;**39**:429–38
- Evans CM, Kim K, Tuvim MJ, Dickey BF. Mucus hypersecretion in asthma: causes and effects. *Curr Opin Pulm Med* 2009;**15**:4–11
- Roth FD, Quintar AA, Uribe Echevarria EM, Torres AI, Aoki A, Maldonado CA. Budesonide effects on Clara cell under normal and allergic inflammatory condition. *Histochem Cell Biol* 2007;**127**:55–68
- Roth FD, Quintar AA, Leimgruber C, Garcia L, Uribe Echevarria EM, Torres AI, Maldonado CA. Restoration of the normal Clara cell phenotype after chronic allergic inflammation. *Int J Exp Pathol* 2013;**94**:399–411
- Hussell T, Bell TJ. Alveolar macrophages: plasticity in a tissue-specific context. *Nat Rev Immunol* 2014;**14**:81–93
- Mosser DM, Edwards JP. Exploring the full spectrum of macrophage activation. *Nat Rev Immunol* 2008;**8**:958–69

22. Dasgupta P, Keegan AD. Contribution of alternatively activated macrophages to allergic lung inflammation: a tale of mice and men. *J Innate Immun* 2012;**4**:478–88
23. Arora S, Olszewski MA, Tsang TM, McDonald RA, Toews GB, Huffnagle GB. Effect of cytokine interplay on macrophage polarization during chronic pulmonary infection with *Cryptococcus neoformans*. *Infect Immun* 2011;**79**:1915–26
24. Strachan DP, Taylor EM, Carpenter RG. Family structure, neonatal infection, and hay fever in adolescence. *Arch Dis Child* 1996;**74**:422–6
25. Liu AH. Hygiene theory and allergy and asthma prevention. *Paediatr Perinat Epidemiol* 2007;**21**:2–7
26. Garn H, Renz H. Epidemiological and immunological evidence for the hygiene hypothesis. *Immunobiology* 2007;**212**:441–52
27. Okada H, Kuhn C, Feillet H, Bach JF. The 'hygiene hypothesis' for autoimmune and allergic diseases: an update. *Clin Exp Immunol* 2010;**160**:1–9
28. Simpson A, Martinez FD. The role of lipopolysaccharide in the development of atopy in humans. *Clin Exp Allergy* 2010;**40**:209–23
29. Takeda M, Tanabe M, Ito W, Ueki S, Konno Y, Chihara M, Itoga M, Kobayashi Y, Moritoki Y, Kayaba H, Chihara J. Gender difference in allergic airway remodelling and immunoglobulin production in mouse model of asthma. *Respirology* 2013;**18**:797–806
30. Szarka RJ, Wang N, Gordon L, Nation PN, Smith RH. A murine model of pulmonary damage induced by lipopolysaccharide via intranasal instillation. *J Immunol Meth* 1997;**202**:49–57
31. Eisenbarth SC, Piggott DA, Huleatt JW, Visintin I, Herrick CA, Bottomly K. Lipopolysaccharide-enhanced, toll-like receptor 4-dependent T helper cell type 2 responses to inhaled antigen. *J Exp Med* 2002;**196**:1645–51
32. Rodriguez D, Keller AC, Faquim-Mauro EL, de Macedo MS, Cunha FQ, Lefort J, Vargaftig BB, Russo M. Bacterial lipopolysaccharide signaling through Toll-like receptor 4 suppresses asthma-like responses via nitric oxide synthase 2 activity. *J Immunol* 2003;**171**:1001–8
33. Henderson WR Jr., Chi EY, Maliszewski CR. Soluble IL-4 receptor inhibits airway inflammation following allergen challenge in a mouse model of asthma. *J Immunol* 2000;**164**:1086–95
34. Zhang X, Goncalves R, Mosser DM. The isolation and characterization of murine macrophages. *Curr Protoc Immunol* 2008;Chapter 14:Unit 14 1
35. Corraliza IM, Campo ML, Soler G, Modolell M. Determination of arginase activity in macrophages: a micromethod. *J Immunol Meth* 1994;**174**:231–5
36. Liu YJ, Soumelis V, Watanabe N, Ito T, Wang YH, Malefyt Rde W, Omori M, Zhou B, Ziegler SF. TSLP: an epithelial cell cytokine that regulates T cell differentiation by conditioning dendritic cell maturation. *Annu Rev Immunol* 2007;**25**:193–219
37. Lambrecht BN, Hammad H. Biology of lung dendritic cells at the origin of asthma. *Immunity* 2009;**31**:412–24
38. Elizur A, Adair-Kirk TL, Kelley DG, Griffin GL, deMello DE, Senior RM. Clara cells impact the pulmonary innate immune response to LPS. *Am J Physiol Lung Cell Mol Physiol* 2007;**293**:L383–92
39. Tang C, Inman MD, van Rooijen N, Yang P, Shen H, Matsumoto K, O'Byrne PM. Th type 1-stimulating activity of lung macrophages inhibits Th2-mediated allergic airway inflammation by an IFN-gamma-dependent mechanism. *J Immunol* 2001;**166**:1471–81
40. Patel NR, Bole M, Chen C, Hardin CC, Kho AT, Mih J, Deng L, Butler J, Tschumperlin D, Fredberg JJ, Krishnan R, Kozziel H. Cell elasticity determines macrophage function. *PLoS ONE* 2012;**7**:e41024
41. Hammad H, Chieppa M, Perros F, Willart MA, Germain RN, Lambrecht BN. House dust mite allergen induces asthma via Toll-like receptor 4 triggering of airway structural cells. *Nat Med* 2009;**15**:410–6
42. Nigo YI, Yamashita M, Hirahara K, Shinnakasu R, Inami M, Kimura M, Hasegawa A, Kohno Y, Nakayama T. Regulation of allergic airway inflammation through Toll-like receptor 4-mediated modification of mast cell function. *Proc Natl Acad Sci U S A* 2006;**103**:2286–91
43. Wang Y, McCusker C. Neonatal exposure with LPS and/or allergen prevents experimental allergic airways disease: development of tolerance using environmental antigens. *J Allergy Clin Immunol* 2006;**118**:143–51
44. Gerhold K, Avagyan A, Seib C, Frei R, Steinle J, Ahrens B, Dittrich AM, Blumchen K, Lauener R, Hamelmann E. Prenatal initiation of endotoxin airway exposure prevents subsequent allergen-induced sensitization and airway inflammation in mice. *J Allergy Clin Immunol* 2006;**118**:666–73
45. Hawrylowicz C, Ryanna K. Asthma and allergy: the early beginnings. *Nat Med* 2010;**16**:274–5
46. Didierlaurent A, Goulding J, Hussell T. The impact of successive infections on the lung microenvironment. *Immunology* 2007;**122**:457–65
47. Holgate ST. The sentinel role of the airway epithelium in asthma pathogenesis. *Immunol Rev* 2011;**242**:205–19

(Received June 24, 2014, Accepted October 20, 2014)